Spin localization, magnetic ordering, and electronic properties of strongly correlated Ln_2O_3 sesquioxides (Ln=La, Ce, Pr, Nd)

Kh. E. El-Kelany,[1,2] C. Ravoux,[1,3] J. K. Desmarais,[1,4,5] P. Cortona,[3] Y. Pan,[4] J. S. Tse,[5] and A. Erba[1,*]

[1]*Dipartimento di Chimica, Università di Torino, Via Giuria 5, 10125 Torino, Italy*

[2]*CompChem Lab, Chemistry Department, Faculty of Science, Minia University, Minia 61519, Egypt*

[3]*Laboratoire Structure Propriétés et Modélisation des Solides (SPMS), CentraleSupélec, Bâtiment G. Eiffel, 3 rue Joliot Curie 91190 Gif-sur-Yvette, France*

[4]*Department of Geological Sciences, University of Saskatchewan, Saskatoon, Canada, SK S7N 5E2*

[5]*Department of Physics and Engineering Physics, University of Saskatchewan, Saskatoon, Canada, SK S7N 5E2*

(Received 22 March 2018; published 12 June 2018)

Lanthanide sesquioxides are strongly correlated materials characterized by highly localized unpaired electrons in the f band. Theoretical descriptions based on standard density functional theory (DFT) formulations are known to be unable to correctly describe their peculiar electronic and magnetic features. In this study, electronic and magnetic properties of the first four lanthanide sesquioxides in the series are characterized through a reliable description of spin localization as ensured by hybrid functionals of the DFT, which include a fraction of nonlocal Fock exchange. Because of the high localization of the f electrons, multiple metastable electronic configurations are possible for their ground state depending on the specific partial occupation of the f orbitals: the most stable configuration is here found and characterized for all systems. Magnetic ordering is explicitly investigated, and the higher stability of an antiferromagnetic configuration with respect to the ferromagnetic one is predicted. The critical role of the fraction of exchange on the description of their electronic properties (notably, on spin localization and on the electronic band gap) is addressed. In particular, a recently proposed theoretical approach based on a self-consistent definition—through the material dielectric response—of the optimal fraction of exchange in hybrid functionals is applied to these strongly correlated materials.

DOI: 10.1103/PhysRevB.97.245118

I. INTRODUCTION

Strongly correlated materials are characterized by unpaired electrons, partially occupying d- or f-type bands, which are strongly interacting and thus tend to be very localized in space to reduce their inter-repulsion [1]. NiO is a prototypical strongly correlated material with the $3d$ band partially occupied and an antiferromagnetic insulating ground state. Rare-earth oxides are strongly correlated materials with a partially occupied $4f$ band that, due to their peculiar electronic properties, are applied as catalysts, dopants for lasers, components of magneto-optic devices, etc. [2,3]. Among them, cerium oxides (ceria) are the most widely used in catalytic applications because of the ease at which cerium sites can be interconverted between trivalent and tetravalent oxidation states [4,5]. Cerium can indeed form both the dioxide CeO_2 (with Ce^{4+} cations with an f^0 empty band) and the sesquioxide Ce_2O_3 (with Ce^{3+} cations with a localized unpaired electron in the f^1 partially occupied band).

Because of its technological applications and because of its prototypical role as a strongly correlated material with f-f on-site interactions, the electronic properties of Ce_2O_3 have been addressed in many theoretical studies by making use of several different computational techniques (see below for a brief account) [6–17]. The insulating nature of its electronic ground state is now fully understood in terms of a broken-symmetry antiferromagnetic spin configuration with one unpaired electron strongly localized on the $4f$ band of each Ce atom.

A detailed analysis of the ground-state electronic and magnetic properties of other rare-earth sesquioxides Ln_2O_3 (with Ln representing any lanthanide in the series Ln=Pr, Nd, ..., Lu) is still to be addressed. All lanthanides form cubic monoxides [18]. In particular, the half-metallic ferromagnetic semiconductor EuO has generated great interest for spintronics applications through manipulation of its seven unpaired f electrons [19]. Among lanthanides, only Ce, Pr, and Tb form dioxides while all 15 form the sesquioxides, although with different structures (hexagonal, monoclinic, or cubic) [20]. In particular, the light rare-earth sesquioxides crystallize into the A-type hexagonal $P\bar{3}m1$ structure. Owing to the high spatial localization of unpaired electrons on their $4f$ orbitals, rare-earth sesquioxides exhibit a large number of possible on-site electronic configurations and different possible intersite magnetic configurations, which make their characterization a rather challenging task [21].

It is nowadays widely acknowledged that, because of this high on-site electron localization, these systems cannot be accurately described by Kohn-Sham density functional theory (DFT) in its standard local density (LDA) or generalized gradient (GGA) approximations. Indeed, even though plain LDA and GGA were initially claimed to be able to capture the correct insulating nature of the ground state of Ce_2O_3 [12],

*alessandro.erba@unito.it

they were later shown to describe a wrong metallic ground state when all-electron basis sets were used or pseudopotential calculations were performed as corrected for nonlinear core effects [13,14].

In order to correctly describe the ground-state electronic and magnetic properties of such strongly correlated materials, more sophisticated computational approaches are required, which correct for the self-interaction error of plain LDA and GGA formulations and thus allow for a reliable description of itinerant *spd* states and localized f ones at the same time. Several techniques have been used to describe the insulating antiferromagnetic ground state of Ce_2O_3 in the last decade, all characterized by the introduction of additional parameters in the theory: Hubbard site-dependent DFT+U [12,16,22], self-interaction-corrected local-spin-density (SIC-LSD) approach [20], many-body perturbation theory in the G_0W_0@LDA + U and GW_0@LDA + U approaches [21,23], global hybrid functionals [17], and range-separated hybrid functionals [15,24].

In this study, we investigate the electronic and magnetic properties of the ground state of four rare-earth sesquioxides Ln_2O_3 (for Ln=La, Ce, Pr, and Nd).

Several metastable electronic configurations are explicitly explored by constraining the occupation of the f orbitals on the Ln sites in order to find the most stable one. Ferromagnetic (F) and broken-symmetry antiferromagnetic (AF) spin configurations are considered to assess their relative stability. Structural parameters, band gaps, density of states, magnetic moments, and spin densities are analyzed. Results on Ce_2O_3 are consistent with the previous copious literature on that system, which would suggest that the description of Pr_2O_3 and Nd_2O_3 is also reliable.

In the present investigation, global hybrid functionals of the DFT are used, which, among self-interaction-corrected techniques (such as DFT+U or GW@DFT+U or screened-Coulomb hybrids), are characterized by the smallest number—1—of supplementary tunable parameters, with respect to non-SIC formulations: the fraction α of nonlocal Fock exchange included into the exchange-correlation functional. The ground-state properties of strongly correlated materials in general, and Ce_2O_3 in particular, have been shown to largely depend on those extra parameters: (i) the dependence on the U parameter of DFT+U calculations has been rigorously documented in Ref. [16]; (ii) the dependence on U of GW_0@LDA+U calculations has been discussed in Ref. [21]; (iii) the dependence on α of global hybrid calculations has been documented in Ref. [17]. The optimal values of such additional parameters are commonly defined empirically by maximizing the agreement with certain experimentally measured quantities (typically the energy band gap) [25].

In this study, self-consistent hybrid functionals are applied to strongly correlated materials, where an optimal fraction of Fock exchange α is self-consistently defined in an iterative scheme as inversely proportional to the computed static electronic dielectric constant of the system ($\alpha \propto 1/\epsilon_\infty$) [26,27]. Self-consistent hybrids are thus characterized by a system-specific optimal fraction of nonlocal exchange defined in terms of the intrinsic electronic screening of the system, which basically eliminates any additional empirical parameter in the formalism. We show how the results obtained for the electronic properties of rare-earth sesquioxides from different self-consistent hybrid functionals are significantly less dispersed than those obtained from different standard hybrid functionals, and nicely reproduce the experimental trends.

The structure of the paper is as follows: Section II is devoted to the presentation of the adopted computational methodologies and settings; in particular, self-consistent hybrid functionals are described as well as the procedure followed to generate optimized basis sets for lanthanides. Results are discussed in Sec. III; in particular, the partial occupation of the f band in lanthanide sesquioxides is first discussed, followed by an investigation of their most stable magnetic ordering and of the nature of their electronic ground state.

II. COMPUTATIONAL DETAILS

Hybrid DFT calculations are performed with a developmental version of the CRYSTAL17 program where crystalline orbitals are expressed in terms of Bloch functions in turn defined as a linear combination of atom-centered local basis functions [28,29]. Such a linear combination of atomic orbitals (LCAO) approach proves particularly convenient when the evaluation of Fock exchange is needed because of the effective implementation of two-electron exchange integral screening, and for the effective evaluation of dielectric properties.

Different atomic guesses for the partial occupation of the f band by the unpaired electrons are used, which allows for an effective exploration of different metastable electronic configurations proper of strongly correlated materials. In this respect, we have applied the following strategy: for each system, all the possible symmetry-allowed subsets of occupied f-type AOs of the lanthanide centers have been considered. For each of them a full self-consistent field (SCF) procedure is run and the corresponding energy is determined.

The Ln_2O_3 sesquioxides (with Ln=La, Ce, Pr, and Nd) are studied in their A-type hexagonal $P\bar{3}m1$ structure, which exhibits 12 symmetry operators and contains two lanthanides per unit cell. The antiferromagnetic spin ordering implies the breaking of the inversion symmetry and a corresponding reduction of symmetry operators from 12 to 6. Reciprocal space is sampled using a Monkhorst-Pack mesh with a shrinking factor of 6 for the primitive cell of all systems, corresponding to 34 independent **k** points in the irreducible portion of the Brillouin zone. A pruned grid with 1454 angular points and 99 radial points for each angular point is used to calculate the DFT exchange-correlation contribution through numerical integration of the electron density over the unit-cell volume. Thresholds controlling the accuracy of Coulomb and exchange series are set to $10^{-8}, 10^{-8}, 10^{-8}, 10^{-8}, 10^{-20}$ (see the CRYSTAL manual).

All structures are fully relaxed both in their F and AF spin configurations by use of analytical energy gradients [30,31] and by including the Pulay force contribution [32], which goes beyond standard Hellmann-Feynman treatments, typically employed in plane-wave codes. The Pulay force includes a term containing the derivative of the overlap matrix with respect to atomic displacements, which formally vanishes at the basis-set limit, but can be important when working with finite basis sets. A quasi-Newton optimizer is used [33], as combined with the Broyden-Fletcher-Goldfarb-Shanno (BFGS) algorithm for

Hessian updating [34–37]. Convergence is checked on both gradient components and nuclear displacements; the corresponding tolerances on their root-mean-square are here set to 0.0003 and 0.0012 a.u., respectively.

A. Hybrid and self-consistent hybrid DFT calculations

Three standard global hybrid functionals of the DFT are used, characterized by different fractions of nonlocal Fock exchange: B1WC (with $\alpha = 16\%$) [38], B3LYP (with $\alpha = 20\%$) [39], and PBE0 (with $\alpha = 25\%$) [40]. For each system, a self-consistent version of these hybrid functionals is defined (sc-B1WC, sc-B3LYP, and sc-PBE0) where the optimal, system-specific, fraction of Fock exchange α is self-consistently obtained within an iterative procedure from its inverse proportionality to the average static electronic dielectric constant of the system [26].

The procedure, as implemented by one of the present authors in the CRYSTAL17 program [27], starts with a guess for the exchange fraction α (any value in the range from 0 to 1) and with the choice of the adopted exchange-correlation DFT functional. At each iteration n of the procedure, the static electronic dielectric tensor of the system is computed, from which an average dielectric constant $\epsilon_\infty^{(n)}$ is evaluated. At the end of each iteration n, the Fock exchange fraction is updated according to $\alpha = 1/\epsilon_\infty^{(n)}$ and convergence of the whole process is checked on the average dielectric constant (i.e., convergence is reached when ϵ_∞ changes by less than 0.1% between two subsequent iterations). At each iteration, the static electronic dielectric tensor of the system is computed by adopting a coupled-perturbed-Hartree-Fock/Kohn-Sham (CPHF/KS) approach [41], as adapted to periodic systems [42]. The CPHF/KS scheme is a perturbative, self-consistent method that focuses on the description of the relaxation of the crystalline orbitals under the effect of an external electric field. The perturbed wave function is then used to calculate the dielectric properties as energy derivatives [43–47].

For comparison, two plain DFT functionals are also used: the local-density approximation functional [48,49] and the generalized-gradient PBE one [50].

B. Basis sets for lanthanides

All-electron basis sets are typically used in LCAO calculations for light or medium atomic weight elements. However, they clearly do not represent an optimal choice when heavy elements are involved. The use of effective core potentials (ECPs) is preferable in this case as they drastically reduce the overall computational cost of the calculation by accounting at the same time for some scalar relativistic effects.

The peculiar electronic and magnetic properties of strongly correlated lanthanide sesquioxides largely depend on the f-f interactions that need to be explicitly described. To do so, small-core pseudopotentials are needed where the $4f$ orbitals are not included in the ECP and rather left into the valence. Large-core pseudopotential basis sets for lanthanides (with the $4f$ electrons included in the ECP) for solids were devised [51], while a small-core pseudopotential valence basis set was available only for Ce [17].

Within the LCAO approach, a one-electron crystalline orbital $\psi_i(\mathbf{r};\mathbf{k})$ is built as a linear combination of Bloch functions $\phi_\mu(\mathbf{r};\mathbf{k})$, defined in terms of local AOs $\varphi_\mu(\mathbf{r})$ [52]:

$$\psi_i(\mathbf{r};\mathbf{k}) = \sum_\mu a_{\mu,i}(\mathbf{k})\phi_\mu(\mathbf{r};\mathbf{k}), \tag{1}$$

$$\phi_\mu(\mathbf{r};\mathbf{k}) = \sum_{\mathbf{g}} \varphi_\mu(\mathbf{r} - \mathbf{A}_\mu - \mathbf{g})e^{i\mathbf{k}\cdot\mathbf{g}}. \tag{2}$$

Here, $\mathbf{r}$ are the coordinates of the electrons, $\mathbf{k}$ denotes a sampling point in reciprocal space, $\mathbf{A}_\mu$ is the position in the reference cell on which φ_μ is centered, and the summation in Eq. (2) is extended to the set of all lattice vectors $\mathbf{g}$. The AOs are in turn expressed as a linear combination of real spherical Gaussian-type functions (GTFs):

$$\varphi_\mu(\mathbf{r} - \mathbf{A}_\mu - \mathbf{g}) = \sum_j d_j^\lambda G_{l,n}^m\left(\alpha_j^\lambda; \mathbf{r} - \mathbf{A}_\mu - \mathbf{g}\right), \tag{3}$$

where d_j^λ and α_j^λ are fixed coefficients and exponents of the shell λ the AO φ_μ belongs to. The AOs are indeed grouped into shells, involving the same quantum numbers n and/or l. The contraction into shells diminishes the number of individual functions used in the evaluation of one- and two-electron integrals, which greatly improves the computational performance.

For this study, we have devised and optimized a consistent series of small-core basis sets with the $4f$ orbitals in the valence for the whole lanthanide series for solid-state applications [53]. We briefly sketch the procedure that we have used in what follows. We have used basis sets with the format ECP28MWB-$(11s11p7d8f2g)/[4s4p2d3f2g]$, in which scalar relativistic effects are treated with the Wood-Boring Hamiltonian [54,55], and the valence was described by four sp shells, two d shells, three f shells, and two g shells. We started the process by optimizing the d_j^λ coefficients and α_j^λ exponents for s, p, d, and f shells for the isolated atom. The f shells were optimized with a partial occupation corresponding to the Ln^{3+} cation (i.e., to the valence of lanthanides in Ln_2O_3 sesquioxides). The most diffuse exponent of the sp, d, and f shells was then reoptimized in the Ln_2O_3 solid and two g shells were added, which represent the first polarization of the occupied f orbitals. The LCAO scheme implemented in the CRYSTAL program has recently been extended to g-type basis functions by some of the present authors in a developmental version of CRYSTAL17 [56]. For the O atoms, we use a previously reported basis set [57], which we have augmented with two d and one f functions whose exponents have been optimized for each Ln_2O_3 solid.

III. RESULTS AND DISCUSSION

A. Partial occupation of the f band

Lanthanide sesquioxides are strongly correlated materials characterized by a partially occupied f band. As introduced in Sec. II, because of the very localized nature of these unpaired electrons, several metastable electronic configurations are possible depending on the partial occupation of the seven f-type orbitals. In this respect, the correct identification of the most stable configuration is mandatory to get a reliable description of the electronic ground state of these strongly correlated

systems. We start our discussion from the characterization of the partial occupation of the f band for Ln_2O_3 with Ln=Ce, Pr, and Nd (La_2O_3 is not considered here because its electronic ground state is a closed-shell one, with an unoccupied f band) before investigating their electronic band gap and structural properties. The seven f-type orbitals are characterized by an angular quantum number $l = 3$ and can be formally identified as f_m where $m = -l, -l+1, \ldots, l-1, l$ is the corresponding magnetic quantum number.

From a symmetry analysis of the A-type hexagonal $P\bar{3}m1$ structure of lanthanide sesquioxides, it is seen that while f_0, f_{-3}, and f_3 are symmetry independent and can thus be occupied independently, the subsets (f_{-1}, f_1) and (f_{-2}, f_2) are group symmetry-related orbitals (i.e., a partial occupation of f_{-1} would imply an identical partial occupation of f_1, for instance). These symmetry considerations apply to both ferromagnetic and antiferromagnetic configurations.

The insulating electronic ground state of Ce_2O_3 has already been carefully investigated in previous studies, which, however, reported seemingly contradicting results: two studies performed using DFT+U and range-separated hybrid functionals reported on a partial occupation of f_0 and f_{-3} (i.e., of f_{z^3} and $f_{y(3x^2-y^2)}$, in a Cartesian representation) [12,15], while a study performed using global hybrid functionals reported on a partial occupation of f_0 and f_3 (i.e., of f_{z^3} and $f_{x(x^2-3y^2)}$) [17]. In this study, we have explicitly explored all possible symmetry-allowed partial occupations of the f orbitals and converged the corresponding electronic states. We find that both previously reported ground states are correct and that they actually coincide. Indeed, they correspond to the exact same occupation of the f orbitals but simply refer to a different conventional orientation of the lattice with respect to the Cartesian frame. Given that the Ln_2O_3 sesquioxides are hexagonal, the lattice is not orthogonal and the orientation with respect to the Cartesian frame can be arbitrarily chosen. Generally, the **c** axis is aligned to z while two conventional orientations are possible in the orthogonal plane: either (i) **a** parallel to x or (ii) **b** parallel to y. It turns out that when the first convention is used, the ground state of Ce_2O_3 can be represented in terms of partially occupied f_{z^3} and $f_{y(3x^2-y^2)}$ orbitals while when the second convention is used of f_{z^3} and $f_{x(x^2-3y^2)}$ ones. It follows that some attention must always be paid when the occupation of d or f orbitals is explicitly given in terms of their Cartesian representations for nonorthogonal lattices, as the relative orientation of the lattice and the Cartesian frame has to be given. Apart from the most stable state, a second insulating metastable state is found, 0.47 eV higher in energy, followed by several metallic metastable states higher in energy by at least 1.35 eV, which is very consistent with the description of the various metastable states of Ce_2O_3 as reported in the LDA+U study by Jiang *et al.* [21].

We have performed a similar detailed analysis on the partial occupation of the f band for the antiferromagnetic ground state of Pr_2O_3 and Nd_2O_3, where each Pr and Nd atom hosts two and three unpaired electrons, respectively. All possible symmetry-independent occupations have been explicitly imposed and constrained-SCF calculations performed. The most stable electronic configuration for Ce_2O_3, Pr_2O_3, and Nd_2O_3 is reported in Table I in terms of the partially occupied f-type orbitals. The most stable solution is given with respect to the two possible conventional orientations of the lattice in the xy plane, that is with **b** ∥ **y** and with **a** ∥ **x**.

TABLE I. The partial occupation of the f band in the most stable electronic configuration of the ground state of Ce_2O_3, Pr_2O_3, and Nd_2O_3, as reported for the two possible conventional orientations of the lattice in the xy plane. For each compound, the list of the partially occupied f orbitals is given; the others are unoccupied.

	Ce_2O_3	Pr_2O_3	Nd_2O_3
b ∥ **y**	$f_{z^3}, f_{(x^2-3y^2)x}$	$f_{xz^2}, f_{yz^2}, f_{(x^2-y^2)z}, f_{xyz}$	$f_{xz^2}, f_{yz^2}, f_{(x^2-3y^2)x}$
a ∥ **x**	$f_{z^3}, f_{(3x^2-y^2)y}$	$f_{xz^2}, f_{yz^2}, f_{(x^2-y^2)z}, f_{xyz}$	$f_{xz^2}, f_{yz^2}, f_{(3x^2-y^2)y}$

B. Magnetic ordering

We now address the issue of the magnetic ordering in lanthanide sesquioxides. In particular, we compute the relative stability of a symmetry-preserving ferromagnetic configuration and a broken-symmetry antiferromagnetic configuration. Five different functionals of the DFT are used: LDA, PBE, and three hybrid ones characterized by different fractions of nonlocal Fock exchange (B1WC, B3LYP, and PBE0).

Plain LDA and GGA functionals were originally reported to predict an insulating antiferromagnetic ground state for Ce_2O_3 [12]. These methods were later shown to describe a metallic ferromagnetic state as the most stable one when all-electron basis sets were used or pseudopotential calculations were performed as corrected for nonlinear core effects, the ferromagnetic solution being more stable than the antiferromagnetic one by about 0.1 eV [13,14]. It was demonstrated that the use of either a $+U$ correction or a fraction of Fock exchange was required to get the correct antiferromagnetic state in Ce_2O_3, which is more stable than the ferromagnetic one by about 3 meV [13,15,17].

Here, the relative stability of the ferromagnetic and antiferromagnetic spin ordering is discussed for Ce_2O_3 (for which detailed comparisons can be made with previously reported descriptions) as well as for Pr_2O_3 and Nd_2O_3, at fixed geometries. The relative stability Δ_{F-AF} (in eV) for the three sesquioxides is reported in Table II as obtained with five different functionals. The description of the relative stability of the different spin configurations that we get for Ce_2O_3 is very consistent with that previously reported: (i) both plain LDA and GGA (PBE in our study) formulations describe a more stable ferromagnetic configuration by about 0.1 eV;

TABLE II. Relative stability $\Delta_{F-AF} = E_F - E_{AF}$ (in eV) of the ferromagnetic and antiferromagnetic spin configurations in Ce_2O_3, Pr_2O_3, and Nd_2O_3 sesquioxides. Results from five different DFT functionals are reported.

	Ce_2O_3	Pr_2O_3	Nd_2O_3
LDA	−0.1442	−0.2812	−0.0187
PBE	−0.1235	−0.0590	−0.0620
B1WC	0.0052	0.0012	0.0001
B3LYP	0.0028	0.0003	0.0005
PBE0	0.0031	0.0007	0.0003

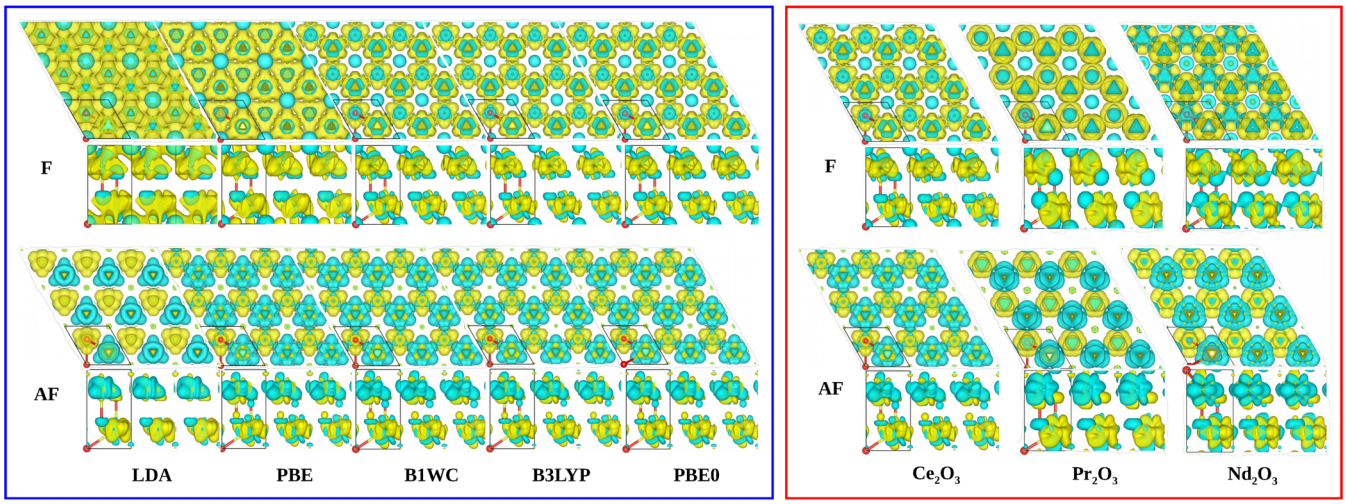

FIG. 1. Left panel: Spin density of Ce_2O_3 as a function of the adopted DFT functional for a F (top) and an AF (bottom) magnetic configuration. Right panel: Spin density of Ce_2O_3, Pr_2O_3, and Nd_2O_3 as obtained with the B1WC hybrid functional. Isodensity surfaces of 0.0015 e/bohr^3 are represented. Yellow and blue surfaces correspond to spin-up and -down electrons, respectively.

(ii) hybrid functionals allow for a correct description of a more stable antiferromagnetic ordering by about 3–5 meV, which is consistent with results of previous DFT + U and range-separated hybrid calculations [13,15,17].

The same overall trend is found also for Pr_2O_3 and Nd_2O_3 where plain DFT functionals predict a stable ferromagnetic ground state while all hybrid functionals provide a stable broken-symmetry antiferromagnetic solution characterized by a smaller relative stability compared to Ce_2O_3 of the order of 0.3–0.7 meV.

C. Spin localization

Because of the high localization of their unpaired f electrons, lanthanide sesquioxides are associated with many different metastable states, often characterized by rather different electronic behaviors (metallic versus insulating, for instance). Thus, an accurate description of the strongly localized f electrons is crucial in order to obtain a reliable description of their electronic properties. Plain LDA and GGA formulations of the DFT provide a wrong metallic solution for the ground state of Ce_2O_3, Pr_2O_3, and Nd_2O_3 while the inclusion of a fraction of nonlocal Fock exchange in hybrid functionals is enough to predict an insulating ground state for all systems. We will discuss in detail the electronic band gap E_g of these systems below. Here, we start by discussing the link between the spin localization (i.e., spatial localization of the unpaired electrons partially occupying the f band) and the observed electronic behavior of the ground-state solution. In particular, we investigate the effect of Fock exchange on spin localization in lanthanide sesquioxides. Despite being crucial, an explicit account of spin localization is seldom given for strongly correlated systems.

The spin density $\sigma(\mathbf{r})$, i.e., difference between the electron density of spin-up and spin-down electrons $\sigma(\mathbf{r}) = \rho^{\alpha}(\mathbf{r}) - \rho^{\beta}(\mathbf{r})$ in scalar relativistic descriptions of Ce_2O_3 is reported in the left panel of Fig. 1 as described by different functionals of the DFT. Both ferromagnetic (F) and antiferromagnetic (AF) configurations are considered. Isovalued surfaces of 0.0015 e/bohr^3 are represented in all cases for ease of comparison. For each case, two views are given: one in the ab plane (top) and one along the c axis (bottom). In Ce_2O_3, each Ce^{3+} ion hosts one unpaired electron in its f band. Plain LDA and GGA formulations are clearly seen to describe rather delocalized unpaired electrons with a higher degree of delocalization in LDA. For instance, in the antiferromagnetic configuration, the integrated magnetic moment on each Ce center is of just $0.61\mu_B$ for LDA and $0.89\mu_B$ for GGA. When a fraction of Fock exchange is included in hybrid functionals, spin localization is greatly enhanced with integrated magnetic moments of $0.97\mu_B$, $0.99\mu_B$, and $0.98\mu_B$ for B1WC, B3LYP, and PBE0 functionals, respectively, thus showing an almost full localization of the unpaired electron on each Ce center. B3LYP is found to be the hybrid functional that provides the most localized description of the f electron. All values of the integrated magnetic moments for the F and AF configurations and for all functionals are given in Table S1 of the Supplemental Material [58], in order to allow for a quantitative analysis of spin localization. Spin localization in the F configuration is consistently found to be higher than in the AF configuration due to higher Pauli repulsion.

The right panel of Fig. 1 shows the evolution of the spin density along the series Ce, Pr, Nd where Ce^{3+}, Pr^{3+}, and Nd^{3+} cations are characterized by one, two, and three unpaired f electrons per center, respectively (the hybrid B1WC functional is used in this case). Table S1 of the Supplemental Material reports the integrated magnetic moments for the three systems and for all functionals. For the AF configuration of Pr_2O_3, for instance, values of $1.88\mu_B$ and $1.96\mu_B$ are obtained at the LDA and GGA level while values of $2.000\mu_B$, $2.004\mu_B$, and $2.001\mu_B$ are found for B1WC, B3LYP, and PBE0 functionals, again confirming the higher localization promoted by Fock exchange. For Nd_2O_3, the spin localization obtained at hybrid level is of $2.992\mu_B$, $2.999\mu_B$, and $2.997\mu_B$ for the three hybrid functionals.

Let us stress that such a detailed description of the electronic state of strongly correlated systems requires special care in their computational description. High control on the initial

TABLE III. Lattice parameters a and c (in Å), c/a ratio, and cell volume V (in Å^3) of Ln_2O_3 in their A-type hexagonal structure for Ln=La, Ce, Pr, Nd, as obtained from full structural relaxations with various functionals and as compared to experimental values taken from Ref. [51]. Relative differences with respect to the experimental values are given within parentheses (in %). For Ln=Ce, Pr, Nd, the computed lattice parameters refer to the AF configuration.

	La_2O_3		Ce_2O_3		Pr_2O_3		Nd_2O_3	
Expt.								
a	3.93		3.89		3.86		3.83	
c	6.14		6.06		6.01		5.99	
V	82.24		79.44		77.55		75.99	
c/a	1.56		1.56		1.56		1.57	
LDA								
a	3.89	(−1.2%)	3.71	(−4.6%)	3.74	(−3.2%)		
c	5.84	(−4.8%)	5.81	(−4.1%)	5.62	(−6.6%)		
V	76.35	(−7.2%)	69.34	(−12.7%)	67.90	(−12.4%)		
c/a	1.50	(−3.6%)	1.57	(0.5%)	1.50	(−3.5%)		
PBE								
a	3.94	(0.2%)	3.85	(−1.1%)	3.80	(−1.5%)	3.76	(−1.7%)
c	6.11	(−0.4%)	6.03	(−0.5%)	5.86	(−2.5%)	5.80	(−3.1%)
V	81.99	(−0.3%)	77.34	(−2.6%)	73.41	(−5.3%)	71.14	(−6.4%)
c/a	1.55	(−0.4%)	1.57	(0.6%)	1.54	(−1.0%)	1.54	(−1.4%)
B1WC								
a	3.90	(−0.8%)	3.84	(−1.4%)	3.80	(−1.5%)	3.74	(−2.3%)
c	5.98	(−2.5%)	5.94	(−2.0%)	5.66	(−5.9%)	5.72	(−4.5%)
V	78.86	(−4.1%)	75.64	(−4.7%)	70.72	(−8.8%)	69.22	(−8.9%)
c/a	1.53	(−1.6%)	1.55	(−0.5%)	1.49	(−4.4%)	1.53	(−2.2%)
B3LYP								
a	3.95	(0.3%)	3.88	(−0.3%)	3.84	(−0.5%)	3.79	(−1.0%)
c	6.22	(1.3%)	6.17	(1.7%)	5.93	(−1.4%)	5.92	(−1.2%)
V	83.85	(2.0%)	80.38	(1.2%)	75.65	(−2.5%)	73.63	(−3.1%)
c/a	1.58	(1.0%)	1.59	(2.1%)	1.55	(−0.8%)	1.56	(−0.1%)
PBE0								
a	3.92	(−0.4%)	3.86	(−0.9%)	3.81	(−1.2%)	3.76	(−1.7%)
c	6.08	(−1.9%)	6.02	(−0.7%)	5.79	(−3.7%)	5.82	(−2.9%)
V	80.80	(−1.8%)	77.55	(−2.4%)	72.93	(−6.0%)	71.32	(−6.1%)
c/a	1.55	(−0.5%)	1.57	(0.3%)	1.52	(−2.5%)	1.55	(−1.2%)

guess for the partial occupation of the f orbitals as well as tools to ensure that the desired electronic configuration is preserved during the SCF procedure are necessary in order to converge these electronic solutions characterized by high spin localization. All states have been converged to 10^{-8} Hartree in the SCF procedure.

D. Structural parameters

Full structural relaxations (atomic positions and lattice parameters) have been performed for La_2O_3, Ce_2O_3, Pr_2O_3, and Nd_2O_3 in their A-type hexagonal $P\bar{3}m1$ structure with the different functionals here considered. For Ce_2O_3, Pr_2O_3, and Nd_2O_3, different structural relaxations have been performed for their ferromagnetic and antiferromagnetic spin configurations. Optimized lattice parameters a, c, c/a ratio, and cell volume V are reported in Table III where they are compared with the experimental values. The volume of lanthanide sesquioxides shrinks along the series. At plain LDA level, a large and systematic underestimation of the cell volume is observed. Also the plain PBE and hybrid B1WC and PBE0 functionals provide a systematic underestimation of the lattice parameters. The B3LYP hybrid functional gives the best description of all structural features. We observe that the different magnetic couplings taking place in the F and AF spin configurations anisotropically affect the structure of lanthanide sesquioxides: the ab plane is almost unaffected by a F $\rightarrow$ AF transformation while the c axis is slightly affected. Lattice parameters for both F and AF configurations are given in Table S2 of the Supplemental Material.

E. Ground-state electronic properties

The lanthanide sesquioxide series exhibits a peculiar nonlinear trend of the band gap E_g, with several minima corresponding to Ce, Eu, Tb, and Yb [24]. A correct and consistent description of this subtle electronic feature represents a challenge to standard DFT methodologies [21]. In particular, the initial sequence of the series (here investigated) presents the deepest minimum, with a band gap of 2.4 eV for Ce_2O_3.

Apart from La_2O_3, which has an empty f band and is characterized by an insulating closed-shell ground-state electronic configuration, the other lanthanide sesquioxides here considered have a partially occupied f band and an

TABLE IV. Electronic energy band gap E_g (in eV) of four lanthanide sesquioxides (in their AF configuration), as computed with different functionals and compared to experimental data (see Ref. [24] and references therein).

	La_2O_3	Ce_2O_3	Pr_2O_3	Nd_2O_3
Expt.	5.3–5.5	2.4	3.5–3.9	4.7–4.8
LDA	3.77	0.00	0.00	0.24
PBE	3.89	0.00	0.00	0.83
B1WC	5.28	2.23	3.33	4.13
B3LYP	5.80	3.43	4.45	4.95
PBE0	6.16	3.75	5.12	5.87

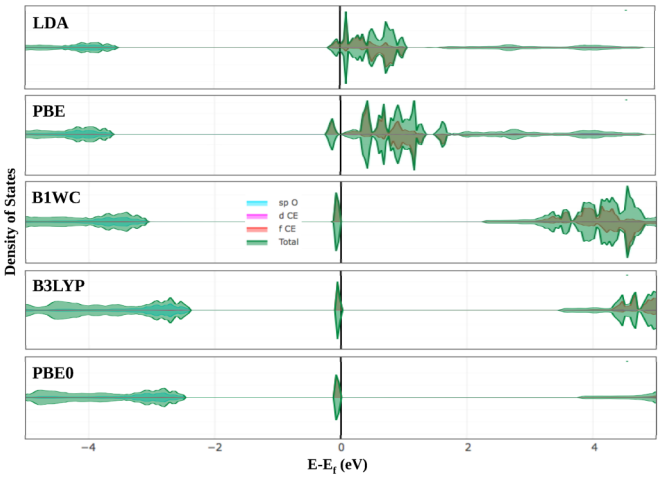

FIG. 2. Electronic density of states of Ce_2O_3 around the Fermi level as computed with different functionals.

open-shell insulating ground-state electronic configuration. As previously reported by many authors, use of either a $+U$ correction or a fraction α of Fock exchange is necessary to "open" a band gap in the electronic structure of Ce_2O_3 with respect to the metallic solution of plain LDA and GGA approaches. This is here confirmed to be the case for Ce_2O_3 and documented to occur also for Pr_2O_3 while plain DFT functionals are found to describe an insulating ground state for La_2O_3 and Nd_2O_3 even if with a too small and incorrect energy band gap. The computed energy band gap E_g of the four sesquioxides here considered is reported in Table IV as obtained with five different functionals and compared to available experimental values. For Ln=Ce, Pr, and Nd, the most stable antiferromagnetic spin configuration is considered.

Plain LDA and GGA functionals of the DFT provide a too low value of about 3.8 eV for the band gap of La_2O_3, compared to an experimental value of about 5.3–5.5 eV. As just said, they provide a metallic description of the ground state of both Ce_2O_3 and Pr_2O_3 and they give very low values of about 0.2 and 0.8 eV for the band gap of Nd_2O_3, whose experimental band gap is of 4.7–4.8 eV. Global hybrid functionals correctly describe the insulating nature of the electronic ground state of all of the four systems. As one changes the hybrid functional, the absolute value of the computed band gap is found to be largely affected: for instance, it passes from 2.23 to 3.75 eV for Ce_2O_3 when passing from B1WC to PBE0 or from 3.33 to 5.12 eV for Pr_2O_3. The electronic density of states around the band gap is given in Fig. 2 for Ce_2O_3 as obtained with different functionals. In order to investigate whether this effect is due to the different fraction of Fock exchange characterizing the different functionals (16% in B1WC, 20% in B3LYP, and 25% in PBE0) or rather to their different GGA part, we have performed calculations by changing the fraction of Fock exchange in the three functionals. Table S3 of the Supplemental Material reports the computed band gap of La_2O_3 as obtained by fixing the fraction of Fock exchange α to the same value for the different hybrid functionals: differences among computed values are never exceeding 0.15 eV. This confirms that the different description of the electronic band gap obtained by different global hybrid functionals is almost entirely due to the different fraction α of exchange and not to their different GGA part.

On the basis of this analysis on the computed values of the band gap from different hybrid functionals in Table IV, an empirical optimization minimizing the difference between computed and experimentally measured electronic band gaps along the lanthanide sesquioxide series would lead to an optimal fraction of Fock exchange of $\alpha = 18\%$. It can be observed from Table IV that among the canonical hybrid functionals used, B1WC overall performs better than the others. In this respect, we might note that among the used functionals, B1WC is the only one that was originally optimized explicitly on periodic systems, while the other ones were originally optimized on molecular systems.

For Ce_2O_3, it is known that the high localization of f electrons is such to create a sharp feature in the electronic density of states in the middle of a wide oxygen $2p$ to cerium $5d$ energy gap [17], which makes the main electronic band gap of the system to be understood as a Ce $4f \rightarrow$ Ce $5d$ one. In order to investigate the "chemical" nature of the band gap in the sesquioxides here considered, we have computed projected densities of states for the various systems in both their F and AF spin configurations. They are reported in Fig. 3 as obtained with the B1WC functional (other hybrid functionals provide a similar description). For all systems, the most stable antiferromagnetic spin configuration is found to exhibit a larger band gap than the corresponding metastable ferromagnetic configuration by about 0.4 eV (see Table S4 in the Supplemental Material for computed band-gap values with all functionals for all systems in their F and AF configurations). For all systems, the top of the valence band is due to the partially occupied f band. As a result of the high electron localization in the stable AF configuration, the f energy band is particularly flat (i.e., shows little dispersion as a function of wave vector $\mathbf{k}$) and thus produces a very localized, sharp feature in the density of states just below the Fermi level.

F. Self-consistent hybrid results

In the previous sections, we have shown that the inclusion of a fraction α of nonlocal Fock exchange in plain DFT functionals represents an effective mean to reach a correct degree of localization of the unpaired f electrons in strongly correlated lanthanide sesquioxides, which proves crucial for a correct description of the insulating antiferromagnetic

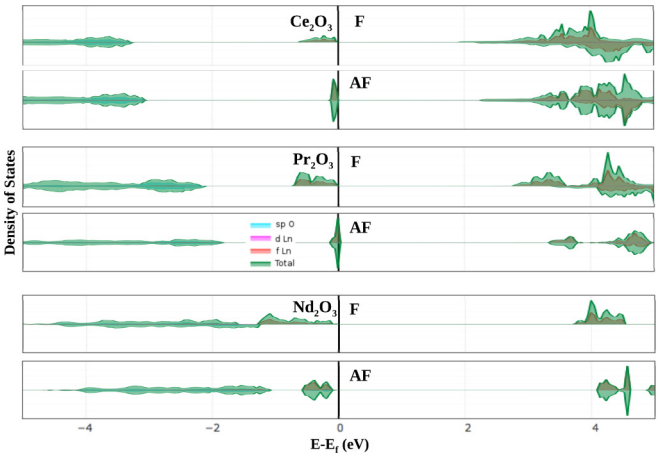

FIG. 3. Electronic density of states (DOS) of Ce_2O_3, Pr_2O_3, and Nd_2O_3 in both their F and AF spin configurations, around the Fermi level as computed with the B1WC hybrid functional. Total (green shadow) and projected (light blue for *sp* band of O, violet for *d* band of Ln, and red for *f* band of Ln) DOS are reported for spin-up and -down electrons above and below the central horizontal line, respectively.

electronic ground state of these systems. On the other hand, we have also shown that many electronic properties (notably the band gap E_g) do largely depend on the particular value of this additional parameter α. This was already carefully documented to be the case for Ce_2O_3 by Graciani *et al.* [17]. As already recalled in the Introduction, a similar critical dependence of computed electronic properties of strongly correlated materials on the additional U parameter in DFT + U calculations has also been documented by several authors [16,21,59].

Several first principles self-consistent approaches have been proposed in the last years to cope with the dependence of self-interaction corrected functionals on their additional parameters [26,27,60–63]. In this study, we apply to strongly correlated materials a recently proposed self-consistent procedure for the definition of an optimal system-specific value of α as inversely proportional to the computed static electronic dielectric constant of the system ($\alpha \propto 1/\epsilon_\infty$), within an iterative procedure [26,27]. For each system, a self-consistent version of the three hybrid functionals considered so far is determined as characterized by a specific value of α (to be referred to as sc-B1WC, sc-B3LYP, and sc-PBE0 in the following discussion). Self-consistent hybrids are thus characterized by a system-specific optimal fraction of nonlocal exchange defined in terms of the intrinsic electronic screening of the system, which basically eliminates any additional empirical parameter in the formalism. The optimal value of α for the various self-consistent hybrids and for each considered system is given in Table V. The effect of the self-consistent definition of α on structural properties is very small, as documented in Table S5 of the Supplemental Material.

We see that, despite that the different hybrid functionals are characterized by very different starting values of α (16%, 20%, and 25%), the self-consistent optimization of this parameter always predict a very similar optimal value for a given system: for La_2O_3 optimal values of 24.6%, 25.5%, and 24.8%, for Pr_2O_3 optimal values of 24.3%, 25.5%, and 24.7%, for instance. This proves that the use of a self-consistent optimization

TABLE V. Band gap E_g (in eV) of the four lanthanide sesquioxides here considered as computed with three different self-consistent hybrid functionals. The optimal fraction α of nonlocal Fock exchange for each functional and each system is also reported.

		La_2O_3	Ce_2O_3	Pr_2O_3	Nd_2O_3
	Expt.	5.3–5.5	2.4	3.5–3.9	4.7–4.8
E_g	sc-B1WC	6.06	3.34	4.89	5.09
	sc-B3LYP	6.29	3.84	5.38	5.33
	sc-PBE0	6.15	3.53	5.07	5.19
α	sc-B1WC	24.6	23.0	24.3	28.9
	sc-B3LYP	25.5	24.1	25.5	29.9
	sc-PBE0	24.8	23.3	24.7	29.1

of the α parameter allows us to obtain an optimal value almost independently of the specific nature of the standard hybrid functional used as a starting guess. This point has a crucial implication: the possibility of defining, for each system, a single optimal value of the α parameter by means of theoretical arguments without the need to define it empirically by comparing to experimental quantities (such as the measured optical band gap).

When use is made of different self-consistent hybrid functionals, the computed values of the electronic properties of the ground state of the system are much less scattered than they are when using different canonical hybrid functionals. This is documented in the upper part of Table V. For instance, for La_2O_3, a maximum deviation of 0.2 eV is found among self-consistent hybrids compared to 0.9 eV among standard hybrids (see Table IV); for Nd_2O_3 a maximum deviation of 0.2 eV among self-consistent hybrids compared to 1.7 eV for standard ones. The computed values of the band gap E_g obtained from self-consistent hybrid functionals are here found to overestimate the experimental values but they do so in a consistent, systematic way and are thus able to reproduce the correct nonlinear trend of the band gap in the series with no need for any empirical parametrization. Let us note that a systematic overestimation of the band gap is to be expected as we have not taken spin-orbit coupling effects into account, which are known to decrease the band gap. This is particularly so when spin-orbit coupling is included self-consistently into the electronic solution rather than *a posteriori* [64].

IV. CONCLUSIONS

Electronic and magnetic properties of the first four lanthanide sesquioxides Ln_2O_3, with Ln=La, Ce, Pr, Nd, have been investigated by means of first principles simulations and hybrid functionals of the DFT. These strongly correlated materials are characterized by highly localized electrons in the *f* orbitals of lanthanide atoms, which generate many metastable electronic configurations depending on their partial occupation. All possible such configurations have here been explicitly explored and the most stable one characterized. In particular, seemingly contradicting descriptions for the ground state of Ce_2O_3 previously reported are rationalized and understood in terms of different conventional lattice orientations. Ferromagnetic and antiferromagnetic spin configurations have

been explored and a higher stability of the antiferromagnetic arrangement found for all considered systems, with a relative stability decreasing along the series from Ce to Pr and Nd.

The critical role of the fraction α of exact nonlocal Fock exchange included into hybrid functionals on the description of spin localization and other electronic properties, like the optical bang gap, has been explicitly investigated. On the one hand, the inclusion of a fraction of exchange into plain LDA or GGA functionals is confirmed to be crucial to get the correct description of the insulating antiferromagnetic ground state of these class of strongly correlated materials. On the other hand, the obtained results are largely affected by the particular value of α. Indeed, we have shown that different hybrid functionals provide different descriptions of the electronic properties because of their different fraction of Fock exchange and to a lesser degree because of the different GGA part. This approach self-consistently defines a system-specific optimal fraction of Fock exchange through its inverse proportionality to the dielectric response of the system, thus taking into account the intrinsic electronic screening of the material. This approach is found to predict much less scattered results and provides a consistent methodological mean to the identification of the optimal fraction of exchange to be included, with no need for any empirical parametrization.

ACKNOWLEDGMENT

We acknowledge CINECA Award No. HP10CBWETR under the ISCRA initiative, for the availability of high performance computing resources and support.

[1] P. Rivero, I. de P. R. Moreira, G. E. Scuseria, and F. Illas, Phys. Rev. B **79**, 245129 (2009).
[2] M. V. Ganduglia-Pirovano, A. Hofmann, and J. Sauer, Surf. Sci. Rep. **62**, 219 (2007).
[3] V. V. Afanas'ev, A. Stesmans, C. Zhao, M. Caymax, T. Heeg, J. Schubert, Y. Jia, D. G. Schlom, and G. Lucovsky, Appl. Phys. Lett. **85**, 5917 (2004).
[4] A. Trovarelli, *Catalysis by Ceria and Related Materials* (Imperial College Press, London, 2002).
[5] M. S. Dresselhaus and I. L. Thomas, Nature (London) **414**, 332 (2001).
[6] N. V. Skorodumova, R. Ahuja, S. I. Simak, I. A. Abrikosov, B. Johansson, and B. I. Lundqvist, Phys. Rev. B **64**, 115108 (2001).
[7] N. V. Skorodumova, S. I. Simak, B. I. Lundqvist, I. A. Abrikosov, and B. Johansson, Phys. Rev. Lett. **89**, 166601 (2002).
[8] S. Gennard, F. Corá, and C. R. A. Catlow, J. Phys. Chem. B **103**, 10158 (1999).
[9] J. C. Conesa, J. Phys. Chem. B **107**, 8840 (2003).
[10] N. V. Skorodumova, M. Baudin, and K. Hermansson, Phys. Rev. B **69**, 075401 (2004).
[11] Z. Yang, T. K. Woo, M. Baudin, and K. Hermansson, J. Chem. Phys. **120**, 7741 (2004).
[12] S. Fabris, S. de Gironcoli, S. Baroni, G. Vicario, and G. Balducci, Phys. Rev. B **71**, 041102(R) (2005).
[13] G. Kresse, P. Blaha, J. L. F. Da Silva, and M. V. Ganduglia-Pirovano, Phys. Rev. B **72**, 237101 (2005).
[14] S. Fabris, S. de Gironcoli, S. Baroni, G. Vicario, and G. Balducci, Phys. Rev. B **72**, 237102 (2005).
[15] P. J. Hay, R. L. Martin, J. Uddin, and G. E. Scuseria, J. Chem. Phys. **125**, 034712 (2006).
[16] C. Loschen, J. Carrasco, K. M. Neyman, and F. Illas, Phys. Rev. B **75**, 035115 (2007).
[17] J. Graciani, A. M. Márquez, J. J. Plata, Y. Ortega, N. C. Hernández, A. Meyer, C. M. Zicovich-Wilson, and J. F. Sanz, J. Chem. Theory Comput. **7**, 56 (2011).
[18] E. Murad and D. L. Hildenbrand, J. Chem. Phys. **73**, 4005 (1980).
[19] A. Schmehl, V. Vaithyanathan, A. Herrnberger, S. Thiel, C. Richter, M. Liberati, T. Heeg, M. Röckerath, L. F. Kourkoutis, S. Mühlbauer *et al.*, Nat. Mater. **6**, 882 (2007).
[20] L. Petit, A. Svane, Z. Szotek, and W. M. Temmerman, Phys. Rev. B **72**, 205118 (2005).
[21] H. Jiang, P. Rinke, and M. Scheffler, Phys. Rev. B **86**, 125115 (2012).
[22] D. Richard, E. L. Muñoz, M. Rentería, L. A. Errico, A. Svane, and N. E. Christensen, Phys. Rev. B **88**, 165206 (2013).
[23] H. Jiang, R. I. Gomez-Abal, P. Rinke, and M. Scheffler, Phys. Rev. Lett. **102**, 126403 (2009).
[24] R. Gillen, S. J. Clark, and J. Robertson, Phys. Rev. B **87**, 125116 (2013).
[25] T. Bredow and B. Stahl, Chem. Phys. Lett. **695**, 28 (2018).
[26] J. H. Skone, M. Govoni, and G. Galli, Phys. Rev. B **89**, 195112 (2014).
[27] A. Erba, J. Phys.: Condens. Matter **29**, 314001 (2017).
[28] R. Dovesi, A. Erba, R. Orlando, C. M. Zicovich-Wilson, B. Civalleri, L. Maschio, M. Rérat, S. Casassa, J. Baima, S. Salustro *et al.*, WIREs Comput. Mol. Sci. e1360 (2018).
[29] A. Erba, J. Baima, I. Bush, R. Orlando, and R. Dovesi, J. Chem. Theory Comput. **13**, 5019 (2017).
[30] K. Doll, Comput. Phys. Commun. **137**, 74 (2001).
[31] K. Doll, V. R. Saunders, and N. M. Harrison, Int. J. Quantum Chem. **82**, 1 (2001).
[32] P. Pulay, *Ab Initio Methods in Quantum Chemistry, Part II*, edited by K. P. Lawley, Vol. 69 (Wiley, Chichester, 2007), p. 241.
[33] B. Civalleri, Ph. D'Arco, R. Orlando, V. R. Saunders, and R. Dovesi, Chem. Phys. Lett. **348**, 131 (2001).
[34] C. G. Broyden, IMA J. Appl. Math. **6**, 76 (1970).
[35] R. Fletcher, Comput. J. **13**, 317 (1970).
[36] D. Goldfarb, Math. Comput. **24**, 23 (1970).
[37] D. F. Shanno, Math. Comput. **24**, 647 (1970).
[38] D. I. Bilc, R. Orlando, R. Shaltaf, G.-M. Rignanese, J. Íñiguez, and P. Ghosez, Phys. Rev. B **77**, 165107 (2008).
[39] A. D. Becke, J. Chem. Phys. **98**, 5648 (1993).
[40] C. Adamo and V. Barone, J. Chem. Phys. **110**, 6158 (1999).
[41] G. J. B. Hurst, M. Dupuis, and E. Clementi, J. Chem. Phys. **89**, 385 (1988).
[42] B. Kirtman, F. L. Gu, and D. M. Bishop, J. Chem. Phys. **113**, 1294 (2000).
[43] M. Ferrero, M. Rérat, R. Orlando, and R. Dovesi, J. Comput. Chem. **29**, 1450 (2008).
[44] M. Ferrero, M. Rérat, R. Orlando, and R. Dovesi, J. Chem. Phys. **128**, 014110 (2008).

[45] M. Ferrero, M. Rérat, R. Orlando, and R. Dovesi, *Computation in Modern Science and Engineering: Proceedings of the International Conference on Computational Methods in Science and Engineering 2007 (ICCMSE 2007): Volume 2, Parts A and B*, AIP Conf. Proc. No. 963, edited by T. E. Simos and G. Maroulis (AIP, Melville, NY, 2007).
[46] B. Kirtman, V. Lacivita, R. Dovesi, and H. Reis, J. Chem. Phys. **135**, 154101 (2011).
[47] R. Dovesi, R. Orlando, A. Erba, C. M. Zicovich-Wilson, B. Civalleri, S. Casassa, L. Maschio, M. Ferrabone, M. De La Pierre, Ph. D'Arco *et al.*, Int. J. Quantum Chem. **114**, 1287 (2014).
[48] J. C. Slater, Phys. Rev. **81**, 385 (1951).
[49] S. H. Vosko, L. Wilk, and M. Nusair, Can. J. Phys. **58**, 1200 (1980).
[50] J. P. Perdew, K. Burke, and M. Ernzerhof, Phys. Rev. Lett. **77**, 3865 (1996).
[51] J. Yang and M. Dolg, Theor. Chem. Acc. **113**, 212 (2005).
[52] C. Pisani, R. Dovesi, and C. Roetti, *Hartree-Fock Ab Initio Treatment of Crystalline Solids*, Lecture Notes in Chemistry Series Vol. 48 (Springer-Verlag, Berlin, 1988).
[53] All optimized basis sets are available at http://www.crystal.unito.it/basis-sets.php.
[54] X. Cao, M. Dolg, and H. Stoll, J. Chem. Phys. **118**, 487 (2003).
[55] M. Dolg, H. Stoll, and H. Preuss, J. Chem. Phys. **90**, 1730 (1989).
[56] J. Desmarais, A. Erba, and R. Dovesi, Theor. Chem. Acc. **137**, 28 (2018).
[57] M. D. Towler, N. L. Allan, N. M. Harrison, V. R. Saunders, W. C. Mackrodt, and E. Aprà, Phys. Rev. B **50**, 5041 (1994).
[58] See Supplemental Material at http://link.aps.org/supplemental/10.1103/PhysRevB.97.245118 for more data on electronic and structural properties.
[59] V. Cantatore and I. Panas, Condens. Matter **2**, 34 (2017).
[60] H. J. Kulik, M. Cococcioni, D. A. Scherlis, and N. Marzari, Phys. Rev. Lett. **97**, 103001 (2006).
[61] H. J. Kulik and N. Marzari, J. Chem. Phys. **129**, 134314 (2008).
[62] M. Cococcioni and S. de Gironcoli, Phys. Rev. B **71**, 035105 (2005).
[63] M. Gerosa, J. Phys.: Condens. Matter **30**, 230301 (2018).
[64] W. P. Huhn and V. Blum, Phys. Rev. Mater. **1**, 033803 (2017).